2013. The Journal of Arachnology 41:184–196

Morphological phylogenetic analysis of the spider genus *Physocyclus* (Araneae: Pholcidae)

Alejandro Valdez-Mondragón: Colección Nacional de Arácnidos (CNAN), Departamento de Zoología, Instituto de Biología, Universidad Nacional Autónoma de México (UNAM). 3er. Circuito exterior s/n. Apartado Postal 70-153, C.P. 04510, Ciudad Universitaria, Coyoacán, Distrito Federal, México. E-mail: lat_mactans@yahoo.com.mx

Abstract. With 30 species and a natural distribution in North America, 28 confined to Mexico, *Physocyclus* Simon 1893 is the most diverse genus within the pholcid spider subfamily Arteminae. This paper provides the first phylogenetic test of the genus's monophyly through a cladistic analysis of 54 morphological characters using equal and implied weighting. The equally weighted analysis found 12 most parsimonious trees, whereas the analysis with implied weights varying the concavity values (K = 6–10) found five or six most parsimonious trees. The monophyly of the genus *Physocyclus* is supported by three synaphomorphies: 1) the paired ventral apophysis on the anterior part of the epigynum; 2) the lateral constraints in the middle part of the epigynum; and 3) the arc of the uterus, with a single sclerotized projection on the anterior part. The genus *Physocyclus* contains two clades treated as species groups: the *globosus* group, with 11 species, and the *dugesi* group with 19 species. The species relationships within the *globosus* group were better resolved than those in the *dugesi* group. The *globosus* group has a biogeographical distribution pattern in the Mesoamerican and Mexican Mountain biotic components, whereas the *dugesi* group has a distribution pattern in the Mesoamerican and Continental Nearctic biotic components. Given the complex biogeography in Mexico, apparently a large-scale vicariant event separated the two major clades within the genus *Physocyclus*.

Keywords: Cladistic analyses, morphology, species groups

The spider family Pholcidae ranks among the most diverse of web-building spider families, currently with 90 genera and 1330 species (Platnick 2013). These spiders are found in temperate, tropical and subtropical forests, with numerous synanthropic species and often in geographic areas and habitats that are severely threatened by human activity (Huber 2000, 2011b). In the New World, a great number of species remain unknown (Gertsch 1982; Huber 1997, 1998, 2000). Huber's (2000) paper is the most complete work for the New World pholcids, particularly from South America. For North America, including Mexico, the principal taxonomic contributions were made by Gertsch (1971, 1973, 1982), Gertsch and Davis (1937, 1942), and Gertsch and Mulaik (1940). Lately, the most recent important taxonomic contributions for North America were made by Slowik (2009) with the taxonomic revision of the genus *Psilochorus* Simon 1893 and Valdez-Mondragón (2010, 2013) with the taxonomic revisions of *Physocyclus* Simon 1893 and *Ixchela* Huber 2000, respectively. Huber (2000) described and redescribed some genera and new species from Mexico. The description of *Modisimus deltoroi* by Valdez-Mondragón and Francke (2009), and the taxonomic revisions of Valdez-Mondragón (2010, 2013), have been the latest taxonomic contributions made for Mexican pholcids. Currently, there has been considerable progress in the knowledge of pholcids from Mexico, with 13 genera and 162 species known.

Despite numerous recent revisions, the diversity of pholcid spiders in the New World is still inadequately known, and many species await description, mostly from previously underrepresented regions of Central and North America (Huber 2000). In Brazil, for example, no fewer than 39 new species were found in the Atlantic Forest (Huber & Rheims 2011), it being one of the most diverse areas in the country. Considerable fieldwork and research at biological collections where many specimens are deposited, not only from Mexico but also from the rest of Central and North America, are also necessary. For example, Valdez-Mondragón (2013) described 10 new species of the genus *Ixchela* Huber 2000 from Mexico and Honduras, and another five are currently being described (A. Valdez-Mondragón unpubl.).

Huber (2011a) divided the family Pholcidae into five subfamilies based on previous cladistic analyses of morphological and molecular data and on qualitative character assessment (Huber 2000; Bruvo-Madarić et al. 2005; Astrin et al. 2006): Ninetinae Simon 1890, Arteminae Simon 1893, Modisiminae Simon 1893, Smeringopinae Simon 1893 and Pholcinae C.L. Koch 1850. Currently, the genus *Physocyclus* is placed within the subfamily Arteminae, which includes 77 species in five genera, with *Physocyclus* and *Trichocyclus* Simon 1908 being the most diverse genera, containing 30 and 23 species respectively (Valdez-Mondragón 2010; Huber 2011a; Platnick 2013). Phylogenetic evidence, both morphological and molecular, suggests a close relationship of *Physocyclus* with *Artema* and *Trichocyclus* (Bruvo-Madarić et al. 2005; Huber 2011a), and the most recent molecular work hypothesizes a sister relationship of *Physocyclus* and *Artema*, a genus distributed in the Middle East (Dimitrov et al. 2013).

The monophyly of *Physocyclus* has never been tested, but now the taxonomic revision of the genus (Valdez-Mondragón 2010), where 13 new species were described, facilitates an analysis of morphological characters based mainly on the homologies within male chelicerae and female epigyna. The primary objective of the present paper is to test the monophyly of the genus and establish the internal relationships among the species through the first cladistic analysis of the genus *Physocyclus*.

METHODS

Biological material.—The specimens used in this study were the same as those examined by Valdez-Mondragón (2010) and are deposited in the following collections: Colección Nacional de Arácnidos (CNAN), Instituto de Biología, Universidad Nacional Autónoma de México, México; Universidad Michoacana de San Nicolás de Hidalgo (UMSNH), Morelia,

Michoacán, México; Centro de Investigaciones Biológicas del Noroeste (CIBNOR), Baja California Sur, México; American Museum of Natural History (AMNH), New York, New York, USA; Texas Memorial Museum (TMM-UT), University of Texas, Austin, Texas, USA; Instituto Nacional de Biodiversidad (INBio), Santo Domingo de Heredia, Costa Rica and Western Australian Museum (WAM), Welshpool, Australia. Other institutions mentioned: California Academy of Sciences (CAS), San Francisco, California, USA; Museum of Comparative Zoology (MCZ), Cambridge, Massachusetts, USA and Muséum National d'Histoire Naturelle, (MNHN) Paris, France. I examined and photographed the specimens with a Nikon SMZ645 stereoscope, following Valdez-Mondragón (2013). The photographs were taken with a Nikon Coolpix S10 VR camera with adapter for the microscope. I used ArcView GIS version 3.2 (Applegate 1999) to prepare distribution maps and edited both the photographs and maps using Adobe Photoshop Version 7.0. Abbreviations used in the figures: E, embolus; ES, embolic sclerites; LAC, lateral apophysis of chelicerae; PP, pore plates; SF, stridulatory files and VAE, ventral apophyses of epigynum.

Taxon sampling.—The cladistic analysis was based on 33 taxa. The ingroup included 29 species of *Physocyclus. Physocyclus mexicanus* Banks 1898 was not included in the analysis because this species is known only from the female holotype, which was not examined. *Physocyclus viridis* Mello-Leitão 1940 (insertae sedis) is known only from the male holotype; however, the characters of the original description seem to belong to another genus and not to *Physocyclus* (Valdez-Mondragón 2010), and furthermore the male holotype is lost (B.A. Huber, pers. comm.). The outgroups included *Priscula binghamae* (Chamberlin 1916), *Trichocyclus nigropunctatus* Simon 1908, *Trichocyclus nullarbor* Huber 2001 and *Artema atlanta* Walckenaer 1837. They were selected based on previous phylogenetic relationships with the family Pholcidae (Huber 2000; Bruvo-Madarić et al. 2005; Astrin et al. 2006; Huber 2011a). The trees were rooted on *P. binghamae,* selected because it belongs to the subfamily Modisiminae, which is phylogenetically related to Arteminae (Huber 2011a).

Character matrix.—The character matrix comprised 54 morphological characters, of which 44 were binary and 10 were multistate (Appendix). Forty-seven characters were informative and seven were uninformative, but they were retained in the matrix because they can potentially contribute to future morphological analyses or taxonomic identification keys. Only the important characters used to diagnose the genus *Physocyclus* and the species groups have been illustrated; for all other characters in the genus *Physocyclus* a recent revision should be consulted (Valdez-Mondragón 2010). In the analyses with equal weighting, I deactivated uninformative characters so as not to inflate the tree length and consistency index (CI). The matrix was maintained in WinClada-Asado, version 1.7 (Nixon 2004). I treated multistate characters as non-additive (Fitch 1971).

Cladistic analysis.—The cladistic analysis with equal weighting was run using Heuristic Search under NONA version 1.8 (Goloboff 1993a) and TNT (Goloboff et al. 2008). In NONA, I conducted the analysis with equal weighting using the following commands: Max trees to keep (hold) = 10,000; No. of replications (mult*N) = 1000; Starting trees per replicate (hold/) = 50; using Multiple TBR+TBR (mult*max*). Under TNT, I conducted the analysis with the following commands: Wagner trees: Random seed = 100; Repls. (Number of add. seqs.) = 10,000; Swapping algorithm: Tree Bisection and Reconnection (TBR); trees to save per replication = 100.

I carried out implied character weighting analyses (Goloboff 1993b, 1995) to assess the effects of weighting against homoplastic characters. In TNT, the analysis with implied weighting was conducted using a traditional search with the following commands: Starting trees (Wagner trees): Random seed = 100; No. of replications = 1000; swapping algorithm (TBR); trees to save per replication = 100. Ten arbitrary values for the concavity constant were used: $K = 1–10$.

Branch support was calculated using Jackknife (Farris et al. 1996) under TNT (Goloboff et al. 2008) and the command: Number of replicates = 1000, removal probability = 36%, using traditional search, and Bremer support (Bremer 1988) under TNT, retain trees suboptimal by 5 steps.

I resolved ambiguous character optimizations with accelerated transformation (ACCTRAN) (Farris 1970; Swofford & Maddison 1987; Agnarsson & Miller 2008). The trees were edited in WinClada and Adobe Photoshop 7.0.

RESULTS

Heuristic equal weighting searches in NONA and TNT found 12 most parsimonious cladograms (L = 127, CI = 70, RI = 85). Figure 1 shows the strict consensus of the minimum length trees in which six nodes collapsed. The cladistic analysis supports the monophyly of the genus *Physocyclus* Simon 1893 with high Jackknife and Bremer values (Fig. 1), and the genus is supported by three synaphomorphies (char. 7, 8, 12) (see discussion for character states). The analysis found two clades within the genus *Physocyclus*, considered as species groups and supported with high Jackknife and Bremer values (Fig. 1). The *globosus* species group consists of 11 species, and the *dugesi* group consists of 19 species (Fig. 1).

The monophyly of the *globosus* group is supported with high Jackknife and Bremer values of 74% and 4 respectively, and by five synapomorphies (Fig. 1): 1) the posterior dorsal sclerotized protuberance on carapace of the female (char. 3) (right arrow, Fig. 14); 2) the sclerotized patch on dorsal anterior part on the female opisthosoma (char. 4) (left arrow, Fig. 14); 3) the short, wide, and oval-shaped pore plates in the epigynum (char. 10, character state 2) (Figs. 17, 21); 4) the dorso-distal spine on the embolus (char. 30) (arrow, Fig. 19) and 5) the embolic sclerites positioned dorsally on the embolus (char. 37) (left arrow, Fig. 15). The monophyly of the *dugesi* group is supported with high Jackknife and Bremer support values of 82% and 5 respectively, and by four synapomorphies (Fig. 1): 1) the lateral constraints in middle part of the epigynum are very marked and bell-shaped (char. 9, character state 1) (arrow, Fig. 2), 2) the embolic sclerites on retrolateral part of the bulb (char. 43) (left arrow, Fig. 8), 3) the notch between embolic sclerites and embolus (char. 45) (middle arrow, Fig. 6) and 4) by having > 30 sclerotized cones frontally on male chelicerae (except *P. platnicki*: Valdez-Mondragón 2010, Fig. 197) (char. 23, character state 1) (Figs. 5, 9).

The analyses with implied weighting, using ten different concavity values (K), also supported the monophyly of the

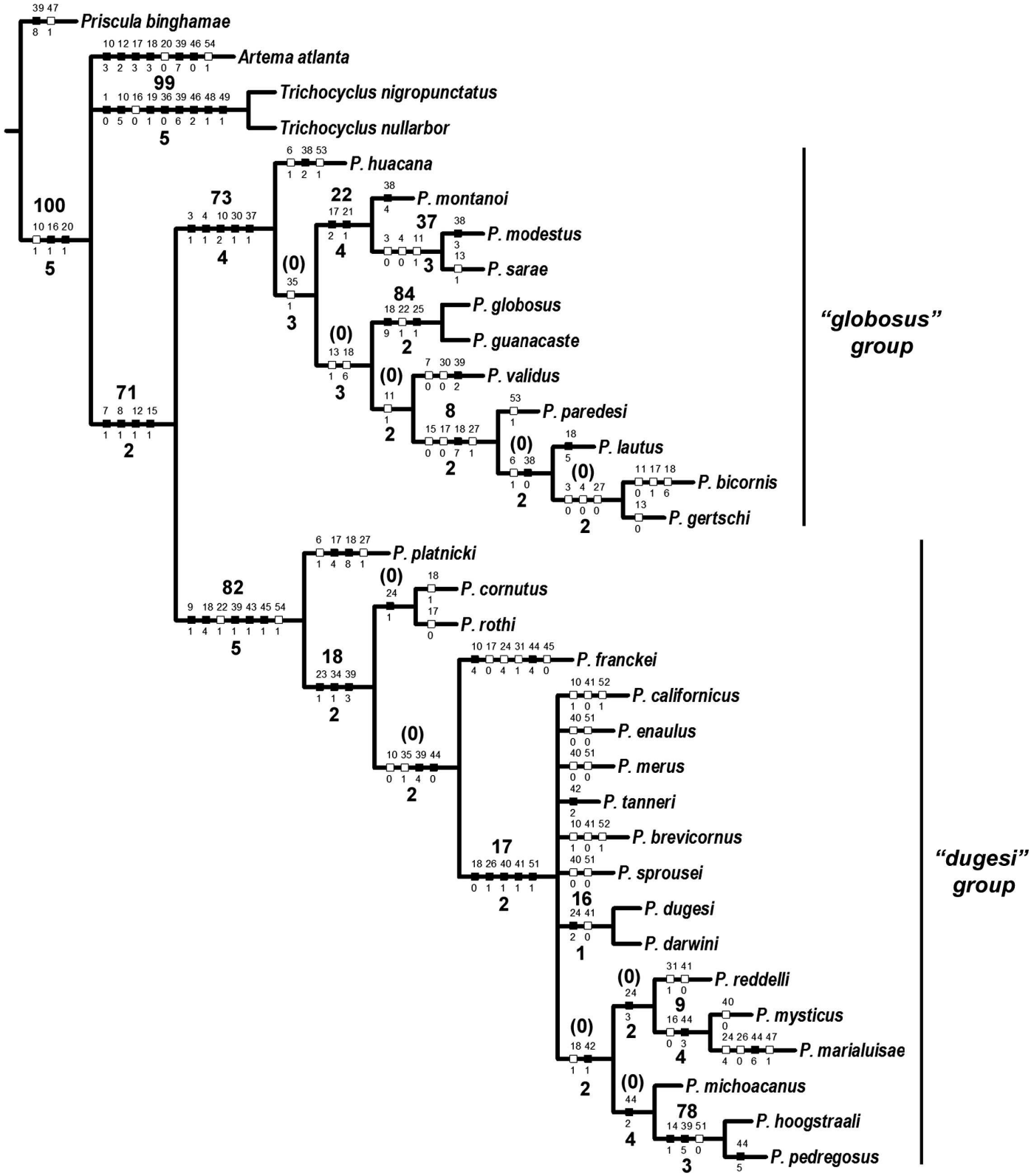

Figure 1.—Strict consensus trees of 12 most parsimonious trees obtained by cladistic analysis with equal weighting of characters under NONA (L= 127, CI=70, RI= 85). Black bars indicate unreversed synapomorphic or apomorphic states, and white bars indicate homoplastic characters. Small numbers above bars indicate character number; small numbers below bars indicate character state. Larger numbers above branches indicate Jackknife support values; larger numbers below branches indicate Bremer support values; (0) above nodes indicate unsupported or collapsed nodes with Jackknife.

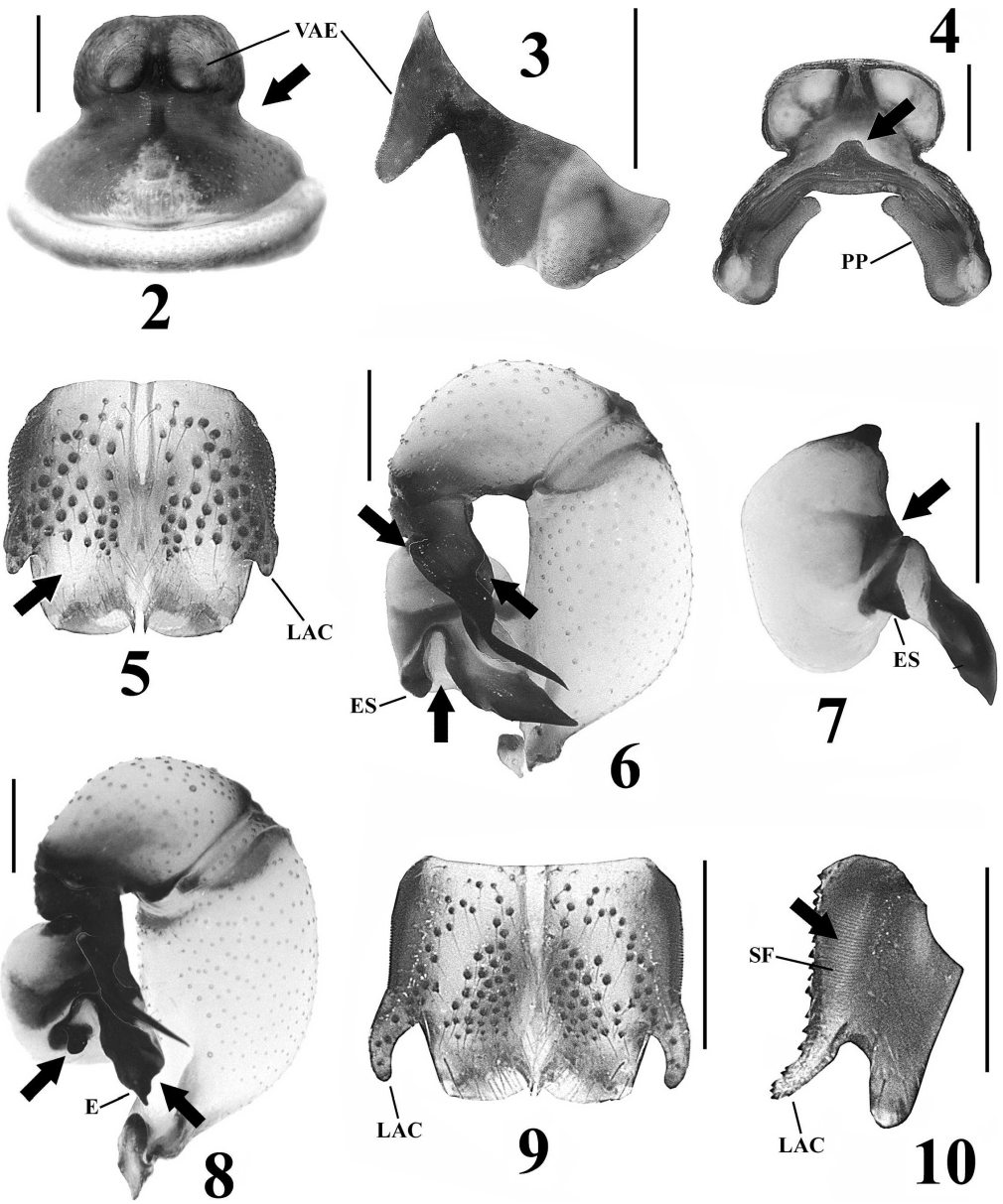

Figures 2–10.—*Physosyclus cornutus*: **2**, **3**. Epigynum, ventral and lateral view respectively (arrow indicates lateral constraints in middle part). *P. michoacanus*: **4**. Epigynum, dorsal view (arrow indicates the single sclerotized projection on the arc). *P. dugesi*: **5**. Chelicerae, frontal view (arrow indicates the pale concavity on each chelicerae); **6**. Left palp, retrolateral view (left arrow indicates dorsal apophysis of procursus; middle arrow indicates the notch between embolic sclerites and embolus; right arrow indicates the ventral notch of the procursus); **7**. Bulb of the left palp, dorsal view (arrow indicates the sclerotized retrolateral region strongly visible). *P. sporusei*: **8**. Left palp, retrolateral view (left arrow indicates the embolic sclerites, right arrow indicates the apical ventral concavity). *P. reddelli*: **9**, **10**. Chelicerae, frontal and lateral views, respectively (arrow indicates the stridulatory file). Scale bars: 0.5 mm.

genus *Physocyclus*, with Jackknife values of ≥ 70 (Table 1). The analyses with concavity values (K = 6–10) obtained fewer parsimonious trees (5 or 6) of the same length as the analysis of equal weighting (Table 1). The analyses with the highest fit values (K = 9, 10) recovered only five parsimonious trees, with the same CI and RI values of the equally weighted trees (Table 1), and the strict consensus found the same topology as with equal weighting (Fig. 1).

Morphological characters.—The morphological characters used in the phylogenetic analysis [54 characters (44 binary and 10 multistate)] are listed below; some characters are described in Valdez-Mondragón (2010), which is abbreviated in this part as VM (2010):

Prosoma:

1. Anterior median eyes, diameter: (0) > diameter of anterior lateral eyes, (1) < diameter of anterior lateral eyes
2. Fovea, shape: (0) point-shaped, (1) longitudinal
3. Carapace of female, posterior dorsal sclerotized protuberance (arrow, Fig. 14): (0) absent, (1) present

Table 1.—Summary of the phylogenetic hypotheses among the most parsimonious trees (MPT) found with equal weighting (EW) and implied weighting (IW), with 10 values for the concavity constant (*K*), arranged in order of increasing fit (*fi*). CI= Consistency index, RI= Retention index, J= Jackknife values that support the monophyly of *Physocyclus* in the different hypothesis.

Analyses	MPT	Steps	fit (*fi*)	CI	RI	Status of *Physocyclus*
IW: *K*= 1	42	133	33.52	67	82	J= 70 (monophyletic)
IW: *K*= 2	14	128	36.97	70	84	J= 71 (monophyletic)
EW	12	127	38.90	70	85	J= 72 (monophyletic)
IW: *K*= 3	14	128	39.10	70	84	J= 72 (monophyletic)
IW: *K*= 4	14	128	40.48	70	84	J= 73 (monophyletic)
IW: *K*= 5	14	128	41.44	70	84	J= 74 (monophyletic)
IW: *K*= 6	5	127	42.17	70	85	J= 74 (monophyletic)
IW: *K*= 7	6	127	42.73	70	85	J= 75 (monophyletic)
IW: *K*= 8	6	127	43.17	70	85	J= 75 (monophyletic)
IW: *K*= 9	5	127	43.53	70	85	J= 75 (monophyletic)
IW: *K*= 10	5	127	43.83	70	85	J= 76 (monophyletic)

Opisthosoma:

4. Opisthosoma of female, sclerotized patch, on dorsal anterior part (arrow, Fig. 14): (0) absent, (1) present
5. Epigynum, distal paired apophysis, next to epigastric furrow: (0) absent, (1) present
6. Epigynum, two small median U-shaped concavities (VM 2010; Figs. 67, 144): (0) absent, (1) present
7. Epigynum, paired ventral apophysis on anterior part (Figs. 2, 3, 11, 20): (0) absent, (1) present
8. Epigynum, lateral constraints in middle part (Figs. 2, 20): (0) absent, (1) present
9. Epigynum, lateral constraints in middle part, shape: (0) barely visible, inconspicuous (Fig. 20); (1) very marked, bell-shaped (arrow, Fig. 2)
10. Epigynum, pore plates, shape: (0) very long and thin (Fig. 4); (1) long and wide (VM 2010; Figs. 13, 20); (2) short, wide, oval-shaped (Fig. 17); (3) short and thin; (4) triangular; (5) short and curved
11. Pore plates, structures bag-shaped below them (arrow, Fig. 21): (0) absent, (1) present
12. Epigynum, sclerotized arc, dorsal view: (0) without sclerotized projection on anterior part, (1) with a sclerotized projection on anterior part (arrows, Figs. 4, 17), (2) with two sclerotized projections on anterior part
13. Epigynum, dorsal arc surrounding pore plates (Fig. 17): (0) absent, (1) present
14. Epigynum, median protuberances, laterally (VM 2010; Figs. 60, 95): (0) absent, (1) present

Legs:

15. Legs, curved setae in tibiae and metatarsi: (0) absent; (1) present

Chelicerae:

16. Chelicerae of male, lateral apophysis (Figs. 5, 9, 12, 13): (0) absent, (1) present
17. Chelicerae of male, lateral apophysis, location: (0) proximal (Fig. 18), (1) middle part (Fig. 5), (2) frontal-retrolateral (arrow, Fig. 12), (3) along, (4) distally (VM 2010; Fig. 197)
18. Chelicerae of male, lateral apophysis, shape: (0) small and conical (Fig. 5), (1) conical and long (Figs. 9, 10), (2) shield-shaped (Fig. 12), (3) wide and along, (4) wide and projected toward front (VM 2010; Fig. 183), (5) small and triangular (Fig. 18), (6) wide and triangular in lateral view (VM 2010; Figs. 2, 113), (7) wide and with two projections in lateral view (VM 2010; Fig. 141), (8) small, with several cones distally (VM 2010; Figs. 197, 198), (9) small and with irregular shape (Fig. 13)
19. Chelicerae of male, frontal curved apophysis, basally: (0) absent, (1) present
20. Chelicerae of male, stridulatory files laterally (arrow, Fig. 10): (0) absent, (1) present
21. Chelicerae of male, discontinuous files frontally: (0) absent, (1) present, on wide apophysis shield-shaped (arrow, Fig. 12)
22. Chelicerae of male, sclerotized cones frontally (Figs. 5, 9): (0) absent, (1) present
23. Chelicerae of male, sclerotized cones frontally, number on each chelicerae: (0) $<$ 20 cones (Fig. 13), (1) $>$ 30 cones (Figs. 5, 9)
24. Chelicerae of male, $>$ 30 sclerotized cones frontally, position: (0) on basal half, and on prolateral part of chelicerae and lateral apophysis (VM 2010, Fig. 8); (1) on basal half, and on prolateral part of chelicerae and lateral apophysis, leaving a basal zone on prolateral part without cones (VM 2010, Fig. 15); (2) on ¾ of total length, and on prolateral part of chelicerae and lateral apophysis (Fig. 5); (3) on prolateral part, and toward prolateral part of lateral apophysis leaving an area with half-moon shape without cones between them (Fig. 9); (4) scattered throughout (VM 2010; Fig. 119)
25. Chelicerae of male in frontal part, pale basal half and brown distal half (Fig. 13): (0) absent, (1) present
26. Chelicerae of male, pale concavity on each chelicera (arrow, Fig. 5): (0) absent, (1) present
27. Chelicerae of male, frontal distal small apophysis, conical (arrow, Fig. 18): (0) absent, (1) present
28. Chelicerae of male, retrolateral frontal apophysis, near to the fangs (*Priscula binghamae*): (0) absent, (1) present

Palps:

29. Procursus, dorsal apophysis and ventral notch basally (left and right arrows respectively, Fig. 6): (0) absent, (1) present

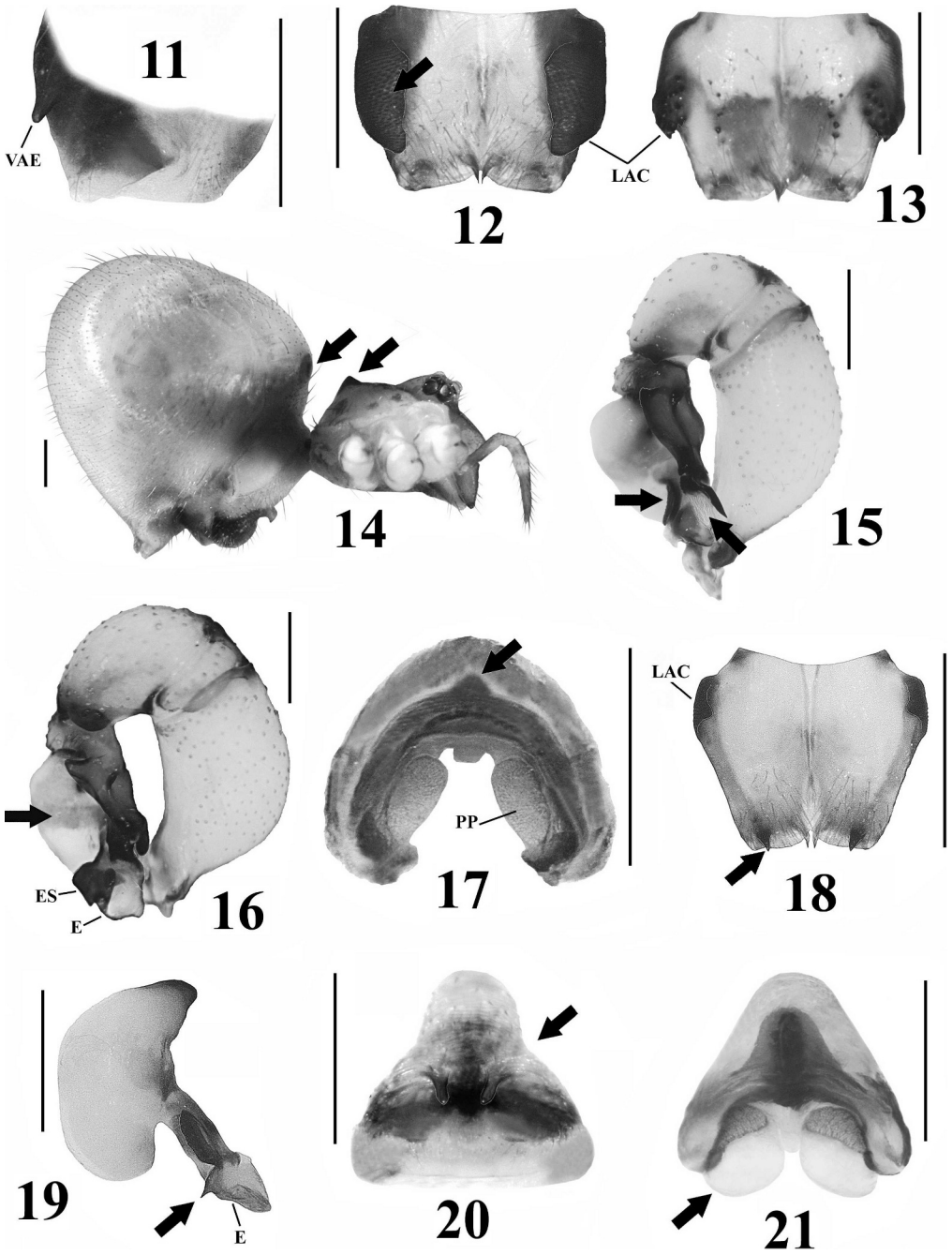

Figures 11–21.—*Physocyclus modestus*: **11**. Epigynum, lateral view; **12**. Chelicerae, frontal view (arrow indicates the frontal-retrolateral apophysis on chelicerae). *P. guanacaste*: **13**. Chelicerae, frontal view. *P. globosus*: **14**. Female habitus, lateral view (left arrow indicates the sclerotized patch on dorsal part of opisthosoma, right arrow indicates the posterior dorsal sclerotized protuberance on carapace); **15**. Left palp, retrolateral view (left arrow indicates the embolic sclerites, right arrow indicates the brush of pseudotrichia on procursus). *P. bicornis*: **16**. Left palp, retrolateral view (left arrow indicates the inconspicuous sclerotized retrolateral region on palp bulb); **17**. Epigynum, dorsal view (arrow indicates the single sclerotized projection on the arc). *P. lautus*: **18**. Chelicerae, frontal view (arrow indicates frontal distal small apophysis); **19**. Bulb of the left palp, dorsal view (arrow indicates the dorso-distal spine on embolus). *P. sarae*: **20.** Epigynum, ventral view (arrow indicates lateral constraints in middle part); **21**. Epigynum, dorsal view (arrow indicates the bag-shaped structures below the pore plates). Scale bars: 0.5 mm.

30. Embolus, dorso-distal spine (arrow, Fig. 19): (0) absent, (1) present
31. Femora of male palp, small prolateral ventral apophysis, with cone-shaped (VM 2010; Fig. 121): (0) absent, (1) present
32. Femora of male palp, prolateral ventral apophysis, distally, oval with flat tip: (0) absent, (1) present
33. Femora of male palp, large ventral conical projection (VM 2010; Fig. 86): (0) absent, (1) present

34. Bulb, sclerotized retrolateral region: (0) absent or inconspicuous (arrow, Fig. 16), (1) strongly visible (arrow, Fig. 7)
35. Procursus, large distal spine (Figs. 6, 8, 15): (0) absent, (1) present
36. Procursus, brush of pseudotrichia distally (right arrow, Fig. 15): (0) absent, (1) present
37. Embolus, embolic sclerites dorsally (left arrow, Fig. 15): (0) absent, (1) present
38. Embolus, embolic sclerites dorsally, shape: (0) large and wide, on almost total length of embolus (VM 2010; Fig. 65); (1) small, on almost total length of embolus, without notch on median part (Fig. 15); (2) long and oval distally, located on basal part of embolus (VM 2010; Fig. 149); (3) small, with notch on median part (VM 2010; Fig. 79); (4) small, projected further than total length of embolus (VM 2010; Fig. 156)
39. Embolus, shape: (0) almost square-shaped distally (Fig. 16); (1) long, with "J"-shape (VM 2010, Fig. 199); (2) long, with upside down "S"-shape (VM 2010; Fig. 114); (3) rounded apically (VM 2010; Fig. 17); (4) triangular-shaped apically (Fig. 6); (5) triangular-shaped dorsally and rounded-shaped ventrally (VM 2010; Fig. 58); (6) conical and oval distally; (7) curved distally; (8) sigmoidal
40. Embolus, with triangular-shaped apically, position: (0) pointing in diagonal position to the longitudinal axis of femur (Fig. 8), (1) pointing in perpendicular position to the longitudinal axis of femur (Fig. 6)
41. Embolus, triangular-shaped apically, with apical ventral concavity (right arrow, Fig. 8): (0) absent, (1) present
42. Embolus, apical ventral concavity, shape: (0) small (right arrow, Fig. 8), (1) curved and long (VM 2010; Fig. 86), (2) circular and large (VM 2010; Fig. 107)
43. Bulb, embolic sclerites on retrolateral part (left arrow, Fig. 8): (0) absent, (1) present
44. Bulb, embolic sclerites on retrolateral part, shape: (0) small and triangular (left arrow, Fig. 8); (1) long and wide (VM 2010; Fig. 17); (2) long and thin (VM 2010; Fig. 58); (3) small and oval (VM 2010; Fig. 86); (4) long and triangular (VM 2010; Fig. 121); (5) small, wide and curved (VM 2010; Fig. 93); (6) long and curved (VM 2010; Fig. 164)
45. Bulb, notch between embolic sclerites and embolus (middle arrow Fig. 6): (0) absent, (1) present
46. Procursus, shape: (0) square (wider than long), (1) conical (wider basally than distally) (Figs. 6, 8, 15, 16), (2) curved (*Trichocyclus*)
47. Male palp, ventral apophysis distally on femur (VM 2010; Fig. 163): (0) absent, (1) present
48. Procursus, long rounded protuberance, ventrally (*Trichocyclus*): (0) absent, (1) present
49. Procursus, dorsal deep concavity (*Trichocyclus*): (0) absent, (1) present
50. Procursus, dorsal projection in middle part (*Priscula*): (0) absent, (1) present
51. Embolus, dorsal projection: (0) absent, (1) present
52. Embolus, dorsal projection, shape: (0) present, curved; (1) present, circular, clearly visible (VM 2010; Fig. 135)
53. Embolus, distal spine (VM 2010; Figs. 149, 206): (0) absent, (1) present
54. Embolus, retrolateral part: (0) white, poorly chitinized (Figs. 15, 16); (1) black, strongly chitinized (Figs. 6, 8)

TAXONOMY

Pholcidae C.L. Koch 1850
Physocyclus Simon 1893

Physocyclus Simon 1893:1(2), 257–488.

Type species.—*Pholcus globosus* Taczanowski 1874:105 (description ♀).

Diagnosis.—Distinguished from other pholcid genera by the combination of the following characters: epigynum with paired ventral apophysis on anterior part (Figs. 2, 3, 11, 20), epigynum with lateral constraints in middle part (arrows, Figs. 2, 20), epigynum with internal sclerotized arc with a sclerotized projection on anterior part (arrows, Figs. 4, 17), male chelicerae with lateral apophysis (Figs. 5, 9, 10, 12, 13), male palp with enlarged femur (Figs. 6, 8, 15, 16), male chelicerae with sclerotized cones frontally (> 30 cones in the *dugesi* group) (Figs. 5, 9). However, cones in the *globosus* group only present on *P. globosus* and *P. guanacaste* (0–20 cones) (Fig. 13).

Description.—Medium-sized spiders (total length 3–7 mm). Carapace usually light yellow, light brown, or with orange undertones, most species with marginal dorsal spots. Fovea with irregular pattern around it, gray or brown. Fovea forming a "Y" with posterior part of ocular region. Eight eyes on ocular region slightly high. Clypeus broad, gently sloping, in some species with two brown, gray or orange lines. Male chelicerae with lateral apophysis (except *P. mysticus* and *P. marialuisae*), apophysis variable in shape and size (Figs. 5, 9, 10, 12, 13, 18). Female chelicerae simple, without apophysis. Male chelicerae with lateral stridulatory files (Fig. 7); females of some species have lateral stridulatory files, but always smaller than the male. Male chelicerae with sclerotized cones on most of the species, variable in number and position (Figs. 5, 9). Male palp femur wide (Figs. 6, 8, 15, 16). Procursus long, dark, sclerotized, with brush of pseudotrichia (right arrow, Fig 15) and spine distally (Figs. 6, 8). Embolic sclerites with different shape and position (arrows, Figs. 8, 15; Valdez-Mondragón 2010, Figs. 10, 51, 72, 93). Embolus in retrolateral part of bulb, sclerotized, with variable shape (Figs. 6–8, 15, 16, 19), sperm duct opening distal-dorsally. Female palp simple. Sternum and labium wider than long, some species have sternum with gray, brown or dark orange spots. Endites long. Males with legs longer than females, femora with rings sub-distally, tibiae with basal and sub-distal rings, more visible in some species than others. Color on legs variable, pale or dark yellow, pale or dark orange, basal part of femora paler than the other segments, metatarsi and tarsi darker than the other segments. Legs without spines. Male legs with curved setae on tibiae and metatarsi. Opisthosoma globular (Fig. 14), thicker than long, larger in females than in males, with lateral and dorsal irregular spots, brown, white or gray. Epigynum with paired anterior ventral apophysis, with variable size and shape (Figs. 2, 3, 11, 20; Valdez-Mondragón 2010, Figs. 5, 33–38). Epigynum wider than long in most species, bell-shaped (Figs. 2, 20; Valdez-Mondragón 2010, Figs. 26, 67, 137). Epigynum with pore plates variable in

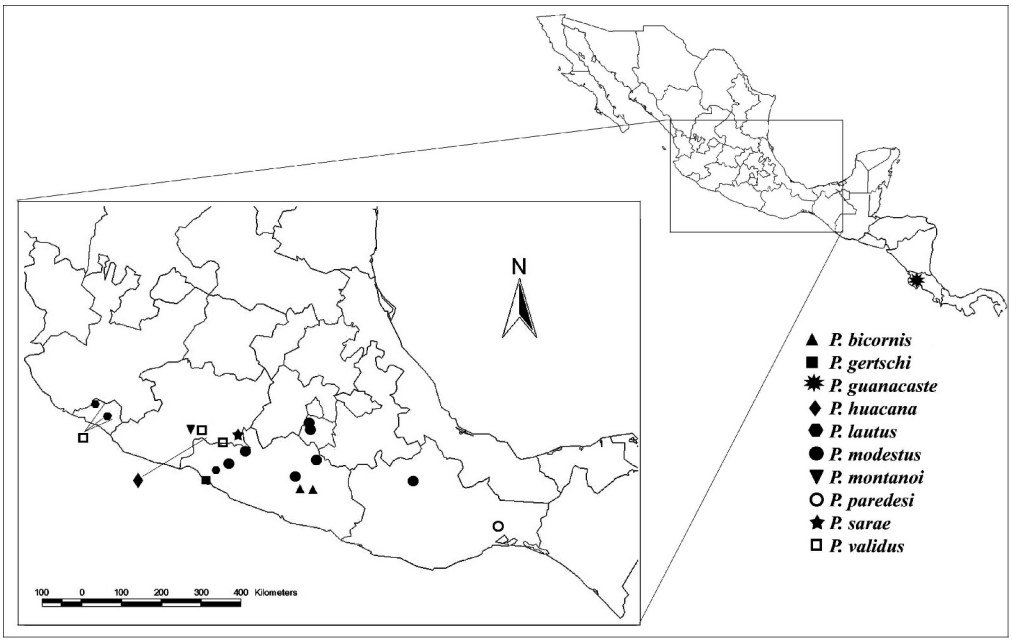

Figure 22.—Natural distribution of the species of the *globosus* group. *Physocyclus globosus* is not plotted because it is introduced in several places around the world.

size, position and shape depending on the species (Figs. 4, 17, 21; Valdez-Mondragón 2010, Figs. 27, 117, 159).

Monophyly.—The genus *Physocyclus* is defined by the following synapomorphies: 1) epigynum with paired ventral apophysis on anterior part (Figs. 2, 3, 11, 20), 2) epigynum with lateral constraints in middle part (arrows, Figs. 2, 20), and 3) epigynum with internal sclerotized arc with a sclerotized projection on anterior part (arrows; Figs. 4, 17).

Composition.—The genus *Physocyclus* is composed of 30 species in two species groups (*globosus* and *dugesi*). The *globosus* group (11 species): *P. globosus* (Taczanowski 1874), *P. bicornis* Gertsch 1971, *P. lautus* Gertsch 1971, *P. modestus* Gertsch 1971, *P. validus* Gertsch 1971, *P. guanacaste* Huber 1988, *P. gertschi* Valdez-Mondragón 2010, *P. huacana* Valdez-Mondragón 2010, *P. montanoi* Valdez-Mondragón 2010, *P. paredesi* Valdez-Mondragón 2010 and *P. sarae* Valdez-Mondragón 2010. The *dugesi* group (19 species): *P. dugesi* Simon 1893, *P. mexicanus* Banks 1898, *P. cornutus* Banks 1898, *P. tanneri* Chamberlin 1921, *P. mysticus* Chamberlin 1924, *P. enaulus* Crosby 1926, *P. californicus* Chamberlin & Gertsch 1929, *P. hoogstraali* Gertsch & Davis 1942, *P. merus* Gertsch 1971, *P. pedregosus* Gertsch 1971, *P. reddelli* Gertsch 1971, *P. brevicornus* Valdez-Mondragón 2010, *P. darwini* Valdez-Mondragón 2010, *P. franckei* Valdez-Mondragón 2010, *P. marialuisae* Valdez-Mondragón 2010, *P. michoacanus* Valdez-Mondragón 2010, *P. platnicki* Valdez-Mondragón 2010, *P. rothi* Valdez-Mondragón 2010 and *P. sprousei* Valdez-Mondragón 2010. Although *P. mexicanus* was not part of the analysis, it was included in *dugesi* group because the female holotype has a long ventral apophysis on the female epigynum as do the other species of the group.

Natural history.—Species such as *P. globosus, P. dugesi* and *P. enaulus* have been collected in houses and buildings (Rodríguez-Márquez & Peretti 2010, Valdez-Mondragón 2010); human activity is responsible for the wide geographic distribution of these species. Synanthropic species occupy corners of ceilings of rooms, basements, bathrooms, under sinks, under tables and benches, under stored items and furniture, and under drains for drainage of roads, in dark warm places without wind currents and with little disturbance. Some species (*P. franckei*, *P. dugesi, P. enaulus, P. hoogstraali*, *P. merus*, *P. pedregosus*, *P. tanneri*, and *P. reddelli*) inhabit dry semiarid climates, while others (*P. huacana, P. modestus, P. validus, P. paredesi, P. bicornis, P. californicus*, *P. cornutus, P. michoacanus, P. brevicornus*, and *P. dugesi*) prefer tropical deciduous forest, between 0–1900 m elevation. Above 1900 m elevation, they have been collected only in buildings. Scientists have never collected the genus in temperate climatic zones such as pine, oak or pine-oak forest, which are the natural habitat for other genera such as *Ixchela* Huber 2000 (Valdez-Mondragón 2013). In karst zones, it is common to find them because of their troglophilic habits; some species have been collected in the entrances of caves and inside on crevices in walls and on formations (stalactites, stalagmites and columns). This is the case for *P. bicornis, P. dugesi, P. enaulus, P. franckei*, *P. hoogstraali*, *P. lautus, P. merus*, *P. modestus*, *P. pedregosus*, *P. reddelli*, *P. tanneri*, and *P. validus*. Outside the caves, their natural habitat is in rock walls, between rocks and dark crevices, with high humidity, warm temperature, and protection from strong wind drafts. Bridges and culverts under roads and railroad tracks are excellent collecting spots.

Distribution.—*Physocyclus* has a natural distribution in North America, with most of the species known found in Mexico (Figs. 22, 23), with *P. californicus, P. enaulus, P. hoogstraali,* and *P. tanneri* distributed in the southern part of the United States, and *P. guanacaste* distributed in Costa Rica. *P. dugesi* has been introduced into Costa Rica and Venezuela, although this last record of Caporiacco (1955) could be

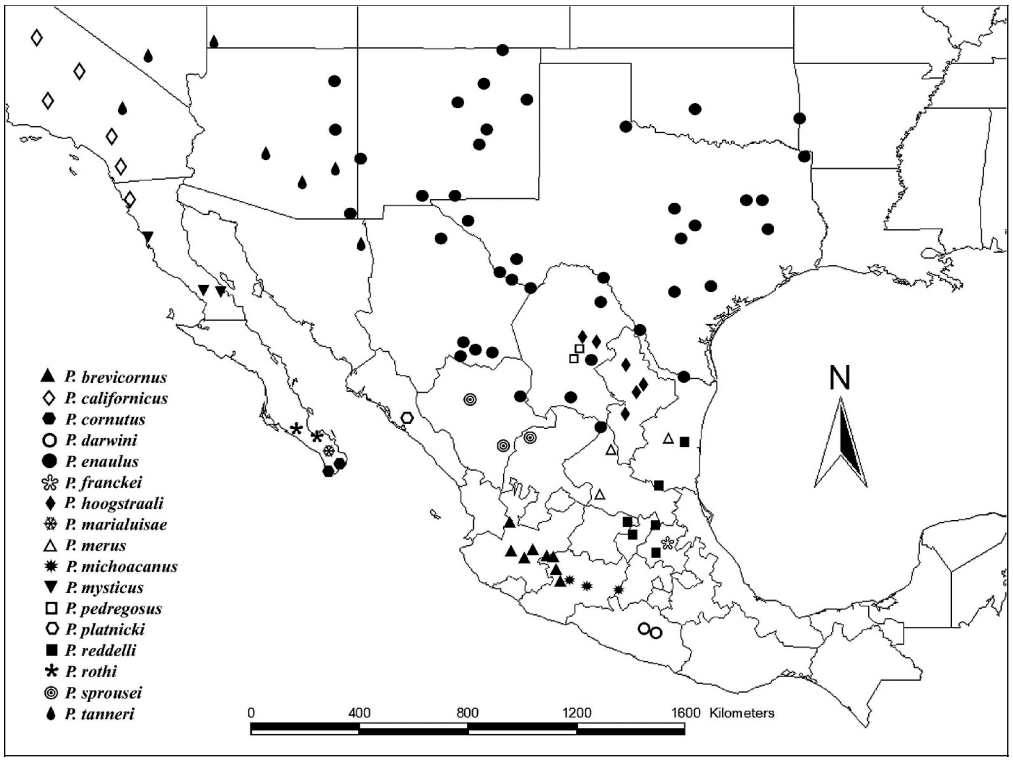

Figure 23.—Natural distribution of the species of the *dugesi* group. *Physocyclus dugesi* is not present because it is an introduced species in Central and South America.

erroneous (B. Huber pers. comm.). *P. globosus* has been introduced and reported in different countries around the world (Valdez-Mondragón 2010).

DISCUSSION

The subfamily Arteminae proposed by Huber (2011) is composed of the genera *Holocneminus*, *Artema, Tibetia, Physocyclus* and *Trichocyclus*; and previous studies have always supported the subfamily (Huber 2001; Bruvo-Madarić et al. 2005). The paired dorsal apophysis and the ventral notch basally on the procursus of the male palp (char. 29) (Huber 2000, 2001) define this subfamily. Recently, Dimitrov et al. (2013), using molecular data, also transferred the genera *Nita* and *Wugigarra* (previously in Modisiminae) to Arteminae. *Wugigarra* also has a paired dorsal apophysis and a basal ventral notch on the procursus of the male palp (B. Huber pers. comm.; A. Valdez-Mondragón pers. obs.), as the do rest of the genera of the subfamily.

In this analysis, I found a trichotomy among *Artema*, *Trichocyclus*, and *Physocyclus* (Fig. 1); Dimitrov et al. (2013) considered *Physocyclus* and *Trichocyclus* to be sister taxa based on the reduction of the epiandrous spigots and preliminary molecular evidence (Huber 2001; Bruvo-Madarić et al. 2005).

The monophyly of the genus *Physocyclus* is supported by three synapomorphies, with high Jackknife and Bremer values that support the genus at 72% and 2 respectively (Fig. 1). The first synapomorphy is the paired ventral apophysis on the anterior part of the epigynum (char. 7) (Figs. 2, 3, 11, 20). However, the apophyses of the species differ in shape, and each species has a particular diagnostic shape. There were two apophysis patterns: conical and short in the *globosus* group (Figs. 11, 20) and long, curved and wide in most of the species in the *dugesi* group (Figs. 2, 3), but these apophyses are absent on *P. validus*, likely a secondary loss (Valdez-Mondragón 2010, Fig. 116). The second character is the lateral constraints in the middle part of the epigynum (char. 8) (arrows, Figs. 2, 20). This character is inconspicuous or barely visible on the species of the *globosus* group (char. 9, character state 0) (Fig. 20), whereas in the *dugesi* group, the shape is very marked (char. 9, character state 1) (Fig. 2). The third character is the arc of the uterus with a single sclerotized projection on its anterior part (char. 12, character state 1) (arrows, Figs. 4, 17), although it is hard to tell if this simple sclerotized projection belongs only to *Physocyclus* or may be present in other genera of Arteminae. At least in *Artema*, this character is present but with two sclerotized projections (char. 12, character state 2), whereas in *Priscula*, *Trichocyclus*, and *Wugigarra* (Huber 2001, Figs. 9, 27, 42), this sclerotized projection is absent. Although the analysis found that a fourth character supporting the monophyly of *Physocyclus* is the curved setae on the tibiae and metatarsi of the legs (char. 15), this character has evolved several times convergently within the subfamilies Arteminae, Modisiminae and Smeringopinae (Huber 2000, 2011). This character was unknown in *P. guanacaste, P. lautus,* and *P. gertschi* due to bad specimen preservation and missing legs, and even these curved setae are absent in *P. paredesi* and *P. bicornis*.

Globosus group*:* The phylogenetic relationships among the species of this group were the same in the 12 most parsimonious trees found in the analysis (Fig. 1). The monophyly of the group is supported by five synapomorphies.

Characters 3 and 4 are a functional unit because these structures are in contact when the female moves its opisthosoma toward the prosoma. However, these characters were coded as different because they were treated as just one character. The analysis found 24 most parsimonious trees, collapsing nine clades with lower values of Ci and Ri. Although the shape of the pore plates is variable in the different species of both groups (char. 10), all species of the *globosus* group share the oval shape (Figs. 17, 21). The dorso-distal spine on the embolus (char. 30) is absent on *P. validus* and can be considered a reversal. In the other species, this spine has different sizes and shapes, which make codification difficult. The dorsal embolic sclerites on the embolus (char. 37) (left arrow, Fig. 15) in the *globosus* group are present on all species. However, the shape of the embolic sclerites (char. 38), which was coded as a multistate character, varies. Only the character state (0): large and wide, almost the total length of the embolus, is shared [*P. lautus* (*P. bicornis* + *P. gertschi*)] (Figs. 1, 16). The large distal spine on the procursus (char. 35) (Figs. 6, 8) is present in all species of the group except *P. huacana*. This character apparently appeared convergently twice, in the *globosus* group (except *P. huacana*) and in most of the species of the *dugesi* group, except *P. platnicki, P. cornutus* and *P. rothi* (Fig. 1).

The clade [*P. montanoi* (*P. modestus* + *P. sarae*)] is supported by the lateral apophysis of male chelicerae in a frontal-retrolateral position (char. 17, character state 2) and male chelicerae with discontinuous files on the wide, shield-shaped apophysis (char. 21, character state 1) (arrow, Fig. 12). This clade had a low Jackknife support value (22%), but a high Bremer support value of 4 (Fig. 1). The position of the lateral apophysis of the male chelicerae was coded as multistate because in both groups the position varies: proximal (character state 0), on the middle part (1), lateral (3) or distally (4). Although the discontinuous files on the apophysis of the male chelicerae support the clade [*P. montanoi* (*P. modestus* + *P. sarae*)], the lateral stridulatory files (char. 20) apparently have evolved convergently several times in different genera of subfamilies Ninetinae, Arteminae and Smeringopinae, except in Modisiminae and Pholcinae (Huber 1995, 2000, 2011a).

Physocyclus globosus + *P. guanacaste* are sister species. Although the shape of the lateral apophysis of the male chelicerae (char. 18) is a multistate character with nine character states, in both species it is small and irregular (character state 9) (Fig. 13). Besides, *P. globosus* + *P. guanacaste* was the only close relationship in the group with high Jackknife and Bremer support values of 84% and 2, respectively (Fig. 1). Another synapomorphy that supports *P. globosus* + *P. guanacaste* is the male chelicerae with a pale basal half and a brown distal half (char. 25) (Fig. 13).

Coding of the apophysis shape of the male chelicerae was difficult due to the variation in the two groups; some of the character states were even autapomorphies for certain species, such as *P. platnicki* and *P. lautus*. This character is also absent in *P. mysticus* and *P. marialuisae* and is considered a reversal. Similarly challenging was the coding of the position of the lateral apophysis of the male chelicerae (char. 17), it being a multistate and homoplastic character (Fig. 1). The bag-shaped structures below each pore plate (char. 11) (arrow, Fig. 21) were found in some species of this group. These structures have apparently evolved convergently twice in the clade *P. modestus* + *P. sarae*, and in the clade composed from *P. validus* to *P. gertschi* (Fig. 1). This character is a reversion in *P. bicornis*.

Although the dorsal embolic sclerites consisted of several shapes (char. 38), they were large and wide for almost the total length of the embolus (character state 0) (Fig. 16), supporting the clade [*P. lautus* (*P. bicornis* + *P. gertschi*)]. In some cases, the character states are diagnostic for such species as *P. modestus*, *P. huacana* and *P. montanoi* (Valdez-Mondragón 2010: Figs. 79, 150, 156). Finally, the conical frontal-distal apophysis on the male chelicerae (char. 27) (arrow, Fig. 18; Valdez-Mondragón 2010, Figs. 197, 204) is a character that may have appeared convergently twice in both species groups because it is present in *P. paredesi* and *P. lautus* (*globosus* group) and *P. platnicki* (*dugesi* group).

Dugesi group*:* In comparison with the *globosus* group, there were changes in the relationships among the species of the *dugesi* group in the 12 most parsimonious trees, with the strict consensus showing the internal relationships in the group (Fig. 1). The monophyly of the group is supported by four synapomorphies. Although the shape of the lateral male chelicerae (char. 18) (Fig. 5, 9, 10) seems to support the group, this character has several character states, one being that the lateral apophysis is small and conical (character state 0) (Fig. 5), the shape that is shared among most of the species (*P. californicus, P. enaulus, P. merus, P. brevicornus, P. sprousei, P. dugesi, P. darwini* and *P. tanneri*). The small, conical lateral apophysis is a plesiomorphic or ancestral state, whereas conical and long (character state 1) (Figs. 9, 10) is a derived state, shared with *P. reddelli, P. michoacanus, P. hoogstraali,* and *P. pedregosus*, but absent on *P. mysticus* and *P. marialuisae* (Valdez-Mondragón 2010; Figs. 84, 161). The embolus shape (char. 39) seems to support the group. However, four different character states were coded, one being an apically triangular embolus (character state 4) (Fig. 6), the state shared in the most of the species except *P. platnicki, P. cornutus, P. rothi, P. hoogstraali*, and *P. pedregosus.* Another character that supports the group is the strongly visible, sclerotized retrolateral region around the male bulb (char. 34, character state 1) (arrow, Fig. 7), absent in *P. platnicki*. About the shape of embolic sclerites on the retrolateral part of bulb (char. 44), apparently the plesiomorphic state was characterized by the species that share long and wide embolic sclerites (character state 1) (Valdez-Mondragón; Figs. 17, 185), whereas the derived state in most of the species was defined by small, triangular embolic sclerites (character state 0) (Figs. 6, 7; left arrow Fig. 8).

Four synapomorphies support the largest clade within the group from *P. californicus* to *P. pedregosus* (Fig. 1); however, this clade is weakly supported with a low Jackknife value of 17%, although supported by with Bremer values of 2. The first synapomorphy is the pale concavity on each chelicera of the male (char. 26) (arrow, Fig. 5) (absent on *P. marialuisae*). The second synapomorphy is the apical position of the triangular-shaped embolus (char. 40); although this is a multistate character, most of the species have a triangular embolus pointing in a perpendicular position to the longitudinal axis of the femur (character state 1) (Fig. 6). Although there is a

polytomy within the relationships of this clade (Fig. 1), this character state might be plesiomorphic, because *P. enaulus, P. merus, P. sprousei*, and *P. mysticus* have the triangular embolus pointing diagonally to the longitudinal axis of the femur (character state 0) (Fig. 8), which could be considered a derived state. This is the same for *P. hoogtraali* + *P. pedregosus* that have an embolus that is triangular dorsally and rounded ventrally (derived state) (char. 39, character state 5) (Valdez-Mondragón 2010; Figs. 58, 93). In species with an apical triangular embolus, the apical ventral concavity on the embolus (char. 41) (right arrow, Fig. 8) in *P. enaulus, P. merus, P. sprousei*, *P. tanneri, P. mysticus, P. marialuisae* and *P. michoacanus* seems to have evolved several times convergently (Fig. 1). The third synapomorphy that seems to support the clade is character 51, the curved dorsal projection on the embolus (Valdez-Mondragón 2010; Fig. 10); however, this character has been lost several times (*P. enaulus, P. merus, P. sprousei*, and *P. hoogtraali* + *P. pedregosus*) (Fig. 8). The fourth synapomorphy is the position of the sclerotized cones of the male chelicerae (char. 24), although most of the species have cones on the basal half and the prolateral part of the chelicerae and lateral apophysis (character state 0) (Valdez-Mondragón 2010; Fig. 29, 70, 105). The plesiomorphic state or ancestral state seems to have cones on the basal half and on the prolateral part of the chelicerae and lateral apophysis, leaving a basal zone on the prolateral part without cones (character state 1), which is present on *P. cornutus* and *P. rothi* (Valdez-Mondragón 2010; Figs. 15, 183). The derived character state consists of cones on the prolateral part and toward the prolateral part of the lateral apophysis, leaving an area of half-moon shape without cones between them (character state 3) on *P mysticus* and *P. reddelli* (Fig. 9); and cones scattered throughout the chelicerae (character state 4) appearing twice convergently on *P. franckei* and *P. marialuisae* (Valdez-Mondragón 2010; Figs. 119, 161).

Finally, the only clade supported with high Jackknife and Bremer values is *P. pedregosus* and *P. hoogstraali*, with 76% and 3 respectively. The characters that support this close relationship include the epigynum with lateral median protuberances (char. 14) (Valdez-Mondragón 2010; Figs. 60, 95) and the dorsally triangular and ventrally rounded embolus (char. 39, character state 5) (Valdez-Mondragón 2010; Figs. 58, 93).

Biogeography.—Analyzing the distribution of the two species groups, I note that the *globosus* group has a distribution in the Mesoamerican and Mexican Mountain biotic components, following the biogeographical scheme of Mexico (Morrone 2004, 2005) (Fig. 22), whereas the *dugesi* group is distributed in the Mesoamerican and Continental Nearctic components (Fig. 23). The biotic components are defined by taxa with a common history, which form biogeographical patterns (Morrone 2005). The biogeography of Mexico is extremely complex; there were several dispersal and vicariance events because Nearctic and the Neotropical biotic elements, known as the Mexican Transition Zone, overlap in Mexico, (Morrone 2005; Brooks 2005). Halffter et al. (1995). Halffter (2003) reviewed this condition, working with the insects of the region.

The Mexican Transition Zone is geographically delimited by the Transmexican Volcanic Belt, a mountain complex in central Mexico (states of Guanajuato, Estado de México, Distrito Federal, Jalisco, Michoacán, Puebla, Oaxaca, Tlaxcala, and Veracruz) (Morrone 2006). By analyzing the distribution of the *globosus* and *dugesi* species groups, I determined that the *globosus* group has a natural distribution primarily toward the south of the Transmexican Volcanic Belt (Neotropical region) (Fig. 22), while the *dugesi* group has a natural distribution toward the north of the Transmexican Volcanic Belt (Nearctic region) (Fig. 23). Given the complex biogeography in Mexico, apparently a large-scale vicariant event separated the two major clades within the genus *Physocyclus* (Fig. 1).

In conclusion, although the genus *Physocyclus* is monophyletic, as are the two species groups within, numerous internal polytomies, mostly within the *dugesi* group, blur a clear phylogenetic picture at the species level. Future studies should use new evidence and add molecular data to help resolve the relationships among the species.

ACKNOWLEDGMENTS

I am grateful to my advisor Dr. Oscar F. Francke for his corrections, guidance, fieldwork support, and comments on the manuscript; to the Instituto de Biología (IBUNAM), Posgrado en Ciencias Biológicas of the UNAM for the education received and to the Consejo Nacional de Ciencia y Tecnología (CONACYT) for the scholarship support during the Masters project and financial support for a visit to the American Museum of Natural History (AMNH), New York, USA, and the Zoologisches Forschungsmuseum Alexander Koenig (ZFAK), Bonn, Germany; to the Richard Gilder Graduate School (AMNH) for the financial support of the Theodore Roosevelt Memorial Fund to study the collection of spiders at the AMNH; to my Master's committee for their advice and great support during the project: Dr. Oscar F. Francke, Dr. José G. Palacios Vargas and Dr. Fernando Álvarez Noguera; to the students of the Colección Nacional de Arácnidos (CNAN) and the Colección Nacional de Ácaros (CNAC) of Instituto de Biología (IBUNAM) for their help during the fieldwork; to Dr. Bernhard A. Huber for his comments and suggestions, which greatly contributed to this work, for the donation of bibliographic material and reception at the ZFAK; to Dr. Norman I. Platnick for his hospitality and help during my visit to the AMNH; to Dr. Maria Luisa Jiménez Jiménez, Dr. Carlos Víquez Nuñez and Dr. Mark Harvey for the loan and donation of biological material; to Nadine Dupérré and Louis Sorkin for their great support during the research visit to the AMNH; to Dr. Matjaž Kuntner and the referees for the comments and suggestions that improved the manuscript; to Carolyn Brown, Sarah Anderson, and Vanessa Reyes from UNAM-Canada for the "Course about Writing Scientific English" (January 7–25, 2013), Institute of Biology, UNAM, Mexico City, Mexico. The specimens were collected under Scientific Collector Permit FAUT-0175 from the Secretaría de Medio Ambiente y Recursos Naturales (SEMARNAT) to Dr. Oscar F. Francke.

LITERATURE CITED

Agnarsson, I. & J.A. Miller. 2008. Is ACCTRAN better than DELTRAN? Cladistics 24:1032–1038.

Applegate, A.D. 1999. ArcView GIS version 3.2. Environmental Systems Research Institute, Inc. Neuron Data, Inc.

Astrin, J.J., B.A. Huber, B. Misof & C.F.C. Klütsch. 2006. Molecular taxonomy in pholcid spiders (Pholcidae: Araneae): evaluation of species identification methods using CO1 and 16S and rRNA. Zoologica Scripta 35:441–457.

Banks, N. 1898. Arachnida from Baja California and other parts of Mexico. Proceedings of the California Academy of Sciences 1:205–308.

Bremer, K. 1988. The limits of amino acid sequence data in angiosperm phylogeny reconstruction. Evolution 42:795–803.

Brooks, D.R. 2005. Historical biogeography and the age of complexity: Expansion and integration. Revista Mexicana de Biodiversidad 76:79–94.

Bruvo-Madarić, B., B.A. Huber, A. Steinacher & G. Pass. 2005. Phylogeny of pholcid spiders (Araneae: Pholcidae): Combined analysis using morphology and molecules. Molecular Phylogenetics and Evolution 37:661–673.

Cambridge, F.O.P. 1902. Arachnida: Araneida and Opiliones. Biologia Centrali-Americana, Zoologia 2:313–424.

Caporiacco, L. di. 1955. Estudios sobre los aracnidos de Venezuela. 2a parte: Araneae. Acta Biológica Venezuelical: 265–448.

Dimitrov, D., J.J. Astrin & B.A. Huber. 2013. Pholcid spider molecular systematics revisited, with new insights into the biogeography and the evolution of the group. Cladistics 29:132–146.

Farris, J.S. 1970. Methods for computing Wagner trees. Systematic Zoology 19:83–92.

Farris, J.S., V.A. Albert, M. Källersjo, D. Lipscomb & A.G. Kluge. 1996. Parsimony jackknifing outperforms neighbour joining. Cladistics 12:99–124.

Fitch, W.M. 1971. Towards defining the course of evolution: Minimal change for a specific tree topology. Systematic Zoology 20:406–416.

Gertsch, W.J. 1971. A report on some Mexican cave spiders. Bulletin of the Association for Mexican Cave Studies 4:47–111.

Gertsch, W.J. 1973. A report on cave spiders from Mexico and Central America. Bulletin of the Association for Mexican Cave Studies 5:141–163.

Gertsch, W.J. 1982. The spider genera *Pholcophora* and *Anopsicus* (Araneae, Pholcidae) in North America, Central America and the West Indies. Texas Memorial Museum Bulletin 28:95–144.

Gertsch, W.J. 1986. The spider genus *Metagonia* (Araneae: Pholcidae) in North America, Central America, and the West Indies. Texas Memorial Museum, Speleological Monographs 1:39–62.

Gertsch, W.J. & L.I. Davis. 1937. Report on a collection of spiders from Mexico. I. American Museum Novitates 961:1–29.

Gertsch, W.J. & L.I. Davis. 1942. Report on a collection of spiders from Mexico. IV. American Museum Novitates 1158:1–19.

Gertsch, W.J. & S. Mulaik. 1940. The spiders of Texas. I. Bulletin of the American Museum of Natural History 77:307–340.

Goloboff, P.A. 1993a. NONA, version 1.8. Computer software and documentation.Online at http://www.cladistics.com

Goloboff, P.A. 1993b. Estimating character weights during tree search. Cladistics 9:83–91.

Goloboff, P.A. 1995. Parsimony and weighting: A reply to Turner and Zandee. Cladistics 11:91–104.

Goloboff, P.A., J.S. Farris & K.C. Nixon. 2008. TNT, a free program for phylogenetic analysis. Cladistics 24:774–786.

Halffter, G. 2003. Biogeografía de montaña de la entomofauna de México y América Central. Pp. 87–97. *In* Una perspectiva latinoamericana de la biogeografía. (J.J. Morrone & J. Llorente-Bousquets, eds.). Las Prensas de Ciencias, UNAM, México, D.F., Mexico.

Halffter, G., M.E. Favila & L. Arellano. 1995. Spatial distributon of three groups of Coleoptera along an altitudinal transect in the Mexican Transition Zone and its biogeographical implications. Elytron 9:151–185.

Huber, B.A. 1995. Copulatory mechanism in *Holocnemus pluchei* and *Pholcus opilionoides*, with notes on male cheliceral apophyses and stridulatory organs in Pholcidae (Araneae). Acta Zoologica (Stockholm) 76:291–300.

Huber, B.A. 1997. Redescriptions of Eugène Simon's neotropical pholcids (Araneae, Pholcidae). Zoosystema 19:573–612.

Huber, B.A. 1998. Notes of the Neotropical spider genus *Modisimus* (Pholcidae, Araneae), with descriptions of thirteen new species from Costa Rica and neighboring countries. Journal of Arachnology 26:19–60.

Huber, B.A. 2000. New World Pholcid Spiders (Araneae: Pholcidae): A revision at generic level. Bulletin of the American Museum of Natural History 254:1–348.

Huber, B.A. 2001. The pholcids of Australia (Araneae; Pholcidae): Taxonomy, biogeography, and relationships. Bulletin of the American Museum of Natural History 260:1–144.

Huber, B.A. 2011a. Phylogeny and classification of Pholcidae (Araneae): an update. Journal of Arachnology 39:211–222.

Huber, B.A. 2011b. Revision and cladistic analysis of *Pholcus* and closely related taxa (Araneae, Pholcidae). Bonner Zoologische Monographien 58:1–509.

Huber, B.A. & C.A. Rheims. 2011. Diversity and endemism of pholcid spiders in Brazil's Atlantic Forest, with descriptions of four new species of the Atlantic Forest endemic genus *Tupigea* (Araneae: Pholcidae). Journal of Natural History 45:275–301.

Morrone, J.J. 2004. Panbiogeografía, componentes bióticos y zonas de transición. Revista Brasileira de Entomologia 48:149–162.

Morrone, J.J. 2005. Hacia una síntesis biogeográfica de México. Revista Mexicana de Biodiversidad 76:207–252.

Nixon, K.C. 2004. WinClada-Asado, version 1.7. Computer software and documentation.Online at http://www.cladistics.com

Nixon, K.C. 1999. The Parsimony Ratchet, a new method for rapid parsimony analysis. Cladistics 15:407–414.

Platnick, N.I. 2013. The world spider catalog, version 13.5. American Museum of Natural History.Online at http://research.amnh.org/iz/spiders/catalog

Rodríguez-Márquez, I.A. & A. Peretti. 2010. Intersexual cooperation during male clasping of external female genitalia in the spider *Physocyclus dugesi* (Araneae, Pholcidae). Journal of Ethology 28:153–163.

Slowik, J. 2009. A review of the cellar spider genus *Psilochorus* Simon 1893 in America north of Mexico (Araneae: Pholcidae). Zootaxa 2144:1–53.

Swofford, D.L. & W.P. Maddison. 1987. Reconstructing ancestral character states under Wagner parsimony. Mathematical Biosciences 87:199–229.

Valdez-Mondragón, A. 2010. Revisión taxonómica de *Physocyclus* Simon, 1893 (Araneae: Pholcidae) con la descripción de especies nuevas de México. Revista Ibérica de Aracnología 18:3–80.

Valdez-Mondragón, A. 2013. Taxonomic revision of the spider genus *Ixchela* Huber, 2000 (Araneae: Pholcidae), with description of ten new species from Mexico and Central America. Zootaxa 3608:285–327.

Valdez-Mondragón, A. & O.F. Francke. 2009. A new species of *Modisimus* (Araneae: Pholcidae) from Chiapas, Mexico. Studies on the cave and endogean fauna of North America. V. Texas Memorial Museum Speleological Monographs 7:57–62.

Manuscript received 16 May 2012, revised 29 March 2013.

Appendix.—Character matrix used in the phylogenetic analyses, composed of 33 taxa (29 ingroup, 4 outgroup), and 54 morphological characters (44 binary and 10 multistate).

Taxa	1	2	3	4	5	6	7	8	9	10	11	12	13	14	15	16	17	18	19	20	21	22	23	24	25	26	27	28	29	30	31	32	33	34	35	36	37	38	39	40	41	42	43	44	45	46	47	48	49	50	51	52	53	54
Priscula binghamae	1	1	0	0	0	0	0	0	-	0	0	0	0	0	0	0	-	-	0	0	0	0	-	-	0	0	0	1	0	0	0	0	0	0	0	1	0	-	8	-	-	-	0	-	-	1	1	0	0	1	0	-	0	0
Artema atlanta	1	0	0	0	0	0	0	0	-	3	0	2	0	0	0	1	3	3	0	0	0	0	-	-	0	0	0	0	1	0	0	0	0	0	0	1	0	-	7	-	-	-	0	-	0	0	0	0	0	0	0	-	0	1
Trichocyclus nigropunctatus	0	1	0	0	0	0	0	0	-	5	0	0	0	0	0	0	-	-	1	1	0	0	-	-	0	0	0	0	1	0	0	0	0	0	0	0	0	-	6	-	-	-	0	-	0	2	0	1	1	0	0	-	0	0
Trichocyclus nullarbor	0	1	0	0	0	0	0	0	-	5	0	0	0	0	0	0	-	-	1	1	0	0	-	-	0	0	0	0	1	0	0	0	0	0	0	0	0	-	6	-	-	-	0	-	0	2	0	1	1	0	0	-	0	0
P. huacana	1	1	1	1	0	1	1	1	0	2	0	1	0	0	1	1	1	2	0	1	0	0	-	-	0	0	0	0	1	1	0	1	0	0	0	1	1	2	0	-	-	-	0	-	0	1	0	0	0	0	0	-	1	0
P. montanoi	1	1	1	1	0	0	1	1	0	2	0	1	0	0	1	1	2	2	0	1	1	0	-	-	0	0	0	0	1	1	0	0	0	0	1	1	1	4	0	-	-	-	0	-	0	1	0	0	0	0	0	-	0	0
P. modestus	1	1	0	0	0	0	1	1	0	2	1	1	0	0	1	1	2	2	0	1	1	0	-	-	0	0	0	0	1	1	0	0	0	0	1	1	1	3	0	-	-	-	0	-	0	1	0	0	0	0	0	-	0	0
P. sarae	1	1	0	0	0	0	1	1	0	2	1	1	1	0	1	1	2	2	0	1	1	0	-	-	0	0	0	0	1	1	0	0	0	0	1	1	1	1	0	-	-	-	0	-	0	1	0	0	0	0	0	-	0	0
P. globosus	1	1	1	1	0	0	1	1	0	2	0	1	1	0	1	1	1	9	0	1	0	1	0	-	1	0	0	0	1	1	0	0	0	0	1	1	1	1	0	-	-	-	0	-	0	1	0	0	0	0	0	-	0	0
P. guanacaste	1	1	1	1	0	0	1	1	0	2	0	1	1	0	?	1	1	9	0	1	0	1	0	-	1	0	0	0	1	1	0	0	0	0	1	1	1	1	0	-	-	-	0	-	0	1	0	0	0	0	0	-	0	0
P. validus	1	1	1	1	0	0	0	1	0	2	1	1	1	0	1	1	1	6	0	1	0	0	-	-	0	0	0	0	1	0	0	0	0	0	1	1	1	1	2	-	-	-	0	-	0	1	0	0	0	0	0	-	0	0
P. paredesi	1	1	1	1	0	0	1	1	0	2	1	1	1	0	0	1	0	7	0	1	0	0	-	-	0	0	1	0	1	1	0	0	0	0	1	1	1	1	0	-	-	-	0	-	0	1	0	0	0	0	0	-	1	0
P. lautus	1	1	1	1	0	1	1	1	0	2	1	1	1	0	?	1	0	5	0	1	0	0	-	-	0	0	1	0	1	1	0	0	0	0	1	1	1	0	0	-	-	-	0	-	0	1	0	0	0	0	0	-	0	0
P. bicornis	1	1	0	0	0	1	1	1	0	2	0	1	1	0	0	1	1	6	0	1	0	0	-	-	0	0	0	0	1	1	0	0	0	0	1	1	1	0	0	-	-	-	0	-	0	1	0	0	0	0	0	-	0	0
P. gertschi	1	1	0	0	0	1	1	1	0	2	1	1	0	0	?	1	0	7	0	1	0	0	-	-	0	0	0	0	1	1	0	0	0	0	1	1	1	0	0	-	-	-	0	-	0	1	0	0	0	0	0	-	0	0
P. platnicki	1	1	0	0	0	1	1	1	1	1	0	1	0	0	1	1	4	8	0	1	0	1	0	-	0	0	1	0	1	0	0	0	0	0	0	1	0	-	1	-	-	-	1	1	1	1	0	0	0	0	0	-	0	1
P. cornutus	1	1	0	0	0	0	1	1	1	1	0	1	0	0	1	1	1	1	0	1	0	1	1	1	0	0	0	0	1	0	0	0	0	1	0	1	0	-	3	-	-	-	1	1	1	1	0	0	0	0	0	-	0	1
P. rothi	1	1	0	0	0	0	1	1	1	1	0	1	0	0	1	1	0	4	0	1	0	1	1	1	0	0	0	0	1	0	0	0	0	1	0	1	0	-	3	-	-	-	1	1	1	1	0	0	0	0	0	-	0	1
P. franckei	1	1	0	0	0	0	1	1	1	4	0	1	0	0	1	1	0	4	0	1	0	1	1	4	0	0	0	0	1	0	1	0	0	1	1	1	0	-	4	0	0	-	1	4	0	1	0	0	0	0	0	-	0	1
P. californicus	1	1	0	0	0	0	1	1	1	1	0	1	0	0	1	1	1	0	0	1	0	1	1	0	0	1	0	0	1	0	0	0	0	1	1	1	0	-	4	1	0	-	1	0	1	1	0	0	0	0	1	1	0	1
P. enaulus	1	1	0	0	0	0	1	1	1	0	0	1	0	0	1	1	1	0	0	1	0	1	1	0	0	1	0	0	1	0	0	0	0	1	1	1	0	-	4	0	1	0	1	0	1	1	0	0	0	0	0	-	0	1
P. merus	1	1	0	0	0	0	1	1	1	0	0	1	0	0	1	1	1	0	0	1	0	1	1	0	0	1	0	0	1	0	0	0	0	1	1	1	0	-	4	0	1	0	1	0	1	1	0	0	0	0	0	-	0	1
P. tanneri	1	1	0	0	0	0	1	1	1	0	0	1	0	0	1	1	1	0	0	1	0	1	1	0	0	1	0	0	1	0	0	0	0	1	1	1	0	-	4	1	1	2	1	0	1	1	0	0	0	0	1	0	0	1
P. brevicornus	1	1	0	0	0	0	1	1	1	1	0	1	0	0	1	1	1	0	0	1	0	1	1	0	0	1	0	0	1	0	0	0	0	1	1	1	0	-	4	1	0	-	1	0	1	1	0	0	0	0	1	1	0	1
P. sprousei	1	1	0	0	0	0	1	1	1	0	0	1	0	0	1	1	1	0	0	1	0	1	1	0	0	1	0	0	1	0	0	0	0	1	1	1	0	-	4	0	1	0	1	0	1	1	0	0	0	0	0	-	0	1
P. dugesi	1	1	0	0	0	0	1	1	1	0	0	1	0	0	1	1	1	0	0	1	0	1	1	2	0	1	0	0	1	0	0	0	0	1	1	1	0	-	4	1	0	-	1	0	1	1	0	0	0	0	1	0	0	1
P. darwini	1	1	0	0	0	0	1	1	1	0	0	1	0	0	1	1	1	0	0	1	0	1	1	2	0	1	0	0	1	0	0	0	0	1	1	1	0	-	4	1	0	-	1	0	1	1	0	0	0	0	1	0	0	1
P. reddelli	1	1	0	0	0	0	1	1	1	0	0	1	0	0	1	1	1	1	0	1	0	1	1	3	0	1	0	0	1	0	1	0	0	1	1	1	0	-	4	1	0	-	1	0	1	1	0	0	0	0	1	0	0	1
P. mysticus	1	1	0	0	0	0	1	1	1	0	0	1	0	0	1	0	-	-	0	1	0	1	1	3	0	1	0	0	1	0	0	0	1	1	1	1	0	-	4	0	1	1	1	3	1	1	0	0	0	0	1	0	0	1
P. marialuisae	1	1	0	0	1	0	1	1	1	0	0	1	0	0	1	0	-	-	0	1	0	1	1	4	0	0	0	0	1	0	0	0	0	1	1	1	0	-	4	1	1	1	1	6	1	1	1	0	0	0	1	0	0	1
P. michoacanus	1	1	0	0	0	0	1	1	1	0	0	1	0	0	1	1	1	1	0	1	0	1	1	0	0	1	0	0	1	0	0	0	0	1	1	1	0	-	4	1	1	1	1	2	1	1	0	0	0	0	1	0	0	1
P. hoogstraali	1	1	0	0	0	0	1	1	1	0	0	1	0	1	1	1	1	1	0	1	0	1	1	0	0	1	0	0	1	0	0	0	0	1	1	1	0	-	5	-	-	-	1	2	1	1	0	0	0	0	0	-	0	1
P. pedregosus	1	1	0	0	0	0	1	1	1	0	0	1	0	1	1	1	1	1	0	1	0	1	1	0	0	1	0	0	1	0	0	0	0	1	1	1	0	-	5	-	-	-	1	5	1	1	0	0	0	0	0	-	0	1